Available online at www.sciencedirect.com
ScienceDirect
Journal of Magnetism and Magnetic Materials 309 (2007) 272–277
Journal of magnetism and magnetic materials
www.elsevier.com/locate/jmmm

Magnetization reversal of ferromagnetic nanoparticles under inhomogeneous magnetic field

Joonyeon Chang[a,*], Hyunjung Yi[a], Hyun Cheol Koo[a], V.L. Mironov[b], B.A. Gribkov[b], A.A. Fraerman[b], S.A. Gusev[b], S.N. Vdovichev[b]

[a]*Nano Device Research Center, Korea Institute of Science and Technology, Seoul 136-791, South Korea*
[b]*Institute for Physics of Microstructures RAS, 603950, GSP-105, Nizhny Novgorod, Russia*

Received 26 October 2005
Available online 7 August 2006

Abstract

We investigated remagnetization processes in ferromagnetic nanoparticles under inhomogeneous magnetic field induced by the tip of magnetic force microscope (MFM) in both theoretical and empirical ways. Systematic MFM observations were carried out on arrays of submicron-sized elliptical ferromagnetic particles of Co and FeCr with different sizes and periods. It clearly reveals the distribution of remanent magnetization and processes of local remagnetization of individual ferromagnetic particles. Modeling of remagnetization processes in ferromagnetic nanoparticles under magnetic field induced by MFM probe was performed on the base of Landau–Lifshitz–Gilbert equation for magnetization. MFM-induced inhomogeneous magnetic field is very effective to control the magnetic state of individual ferromagnetic nanoparticles as well as to create different distribution of magnetic field in array of ferromagnetic nanoparticles.

Keywords: Magnetization reversal; Magnetic force microscopy; Single magnetic domain; Vortex

1. Introduction

Ferromagnetic nanoparticles are basic elements to detect or create magnetic field as well as to record information. [1]. These applications are based on a discrete magnetic state in laterally confined ferromagnetic nanostructures. For example, only uniform states (US) with opposite directions of magnetization are possible in a single-domain anisotropic particle. Vortex state (VS) is realized in a particle with geometrical sizes above critical length [2–5]. US are also possible in such ferromagnetic nanoparticles as metastable states [6]. The reversible change of both magnetic states of ferromagnetic nanoparticles opens up a unique opportunity to use such a system as an artificial source of inhomogeneous magnetic field.

Amplitude of inhomogeneous magnetic field is about the saturation magnetic moment M_s of the ferromagnet and a scale of the field variation is determined by the period of particle array. For typical transition metals, M_s is about 1000 G and the modern lithographic techniques allow one to vary the particle lattice period over a wide range from 10 to 1000 nm. In addition, magnetic field distribution can be varied by magnetizing or demagnetizing the whole particle array or some of its parts.

Influence of controllable inhomogeneous magnetic field induced by the particles leads to drastic change in the transport properties of superconductors [7–10] and Josephson junctions [11–13]. Recently, it was shown that the nonhomogeneous magnetic field produced by the ferromagnetic island acts as an effective potential that can trap spin-polarized carriers in the system with giant Zeeman splitting [14]. Giant G factor was observed, for example, in diluted magnetic semiconductors [15]. Influence of spin injection from ferromagnetic particles on transport properties of superconductors [16–19] and semiconductors [20] is another interesting field for application of ferromagnetic particles.

*Corresponding author. Tel.: +82 2 958 6822; fax: +82 2 958 5431.
E-mail address: presto@kist.re.kr (J. Chang).

0304-8853/$ - see front matter © 2006 Elsevier B.V. All rights reserved.
doi:10.1016/j.jmmm.2006.07.015

One of the possibilities for manipulation of magnetic state of ferromagnetic nanoparticles is magnetization reversal under the probe of MFM. In this case, magnetic state of each selected element can be controlled by approaching the MFM probe to a specific particle independently. In such a way, we can fabricate different distributions of magnetization in an array of ferromagnetic particles, which can be useful for various applications. Moreover, magnetic tip induces inhomogeneous magnetic field and magnetization reversal has additional peculiarities in comparison with the process in uniform external magnetic field. Regardless of the fact that influence of magnetic tip on state of ferromagnetic particles was experimentally investigated earlier [21–24], the problem still needs further study.

In this work, we investigated both theoretically and experimentally remagnetization processes in ferromagnetic nanoparticles under inhomogeneous magnetic field induced by magnetic tip of MFM, which allow to realize inhomogeneous magnetic field sources based on nanoparticle arrays.

2. Experimentals

Rectangular lattices of elliptical ferromagnetic particles with different sizes of elements and different periods were fabricated by electron-beam lithography and subsequent ion etching of thin FeCr or Co films. [14] The unique feature to be noticed here is the use fullerene consisting of C_{60} molecules as a electron beam resist which acts as a patterning media as well as a robust mask for ion etching. The characteristic lateral sizes of particles was $400\,\text{nm} \times 600\,\text{nm}$ (aspect ratio of 1.5) and heights of particles were varied from 10 to 30 nm. Details of the sample preparation were reported in previous work [25].

The distribution of remanent magnetization and processes of local remagnetization were studied using a multimode SPM Solver-PRO (NT-MDT). MFM measurements were performed in the noncontact constant height mode and the standard double pass tapping/lift mode. Standard Co-coated silicon cantilevers (MicroMash) magnetized along the tip axis prior to magnetic imaging were used in the MFM experiments. The phase shift of cantilever oscillations under a gradient of magnetic field was registered as the MFM contrast.

3. Computer simulations

Modeling of remagnetization processes in ferromagnetic nanoparticles under MFM probe magnetic field was performed on the base of Landau–Lifshitz–Gilbert (LLG) equation for magnetization $\vec{M}(\vec{r},t)$:

$$\frac{\partial \vec{M}}{\partial t} = -\frac{\gamma}{1+\alpha^2}[\vec{M}\times\vec{H}_{\text{eff}}] - \frac{\alpha\gamma}{(1+\alpha^2)M_s}[\vec{M}\times[\vec{M}\times\vec{H}_{\text{eff}}]], \quad (1)$$

where γ is the gyromagnetic ratio, α the dimensionless damping parameter and M_s the magnetic moment in saturation. The effective field $\vec{H}_{\text{eff}} = -\delta E/\delta\vec{M}$ is a variation derivative of the energy function. The total energy of the particle can be defined by

$$E = E_{\text{ex}} + E_m + E_h. \quad (2)$$

The first term E_{ex} is the energy of the exchange interaction, the second term E_m is the demagnetization energy of the particles. Expressions for these terms have the conventional form [15]. The last term E_{h} is the energy of the interaction between the magnetic moment and the non-uniform external magnetic field $\vec{H}$. In calculations the MFM probe was approximated as a single dipole [16,17] with effective magnetic moment $m_{\text{eff}} = M_{\text{sp}}V_{\text{eff}}$ (M_{sp} is the remanent magnetization of capping material, V_{eff}—the effective volume of the interactive part of magnetic layer). We studied redistribution of magnetization during probe moving across the particles. At the each stage stationary solutions of the LLG equations for the particles in the inhomogeneous field of MFM probe have been found for selected probe positions. Afterwards the probe has been replaced in the next position and LLG equations have been solved again with previous magnetization distribution used as the initial state for the next step computation.

To avoid a three-dimensional grid problem, which needs large computer resources, we assumed that magnetization of a cylindrical particle does not depend on the coordinate z along the cylindrical axis. Then we integrated the relations for the energy over z and obtained the energy as a function of the magnetization, which is a function of only two space variables. The effective field $\vec{H}_{\text{eff}}$ does not depend on z either, so we have a three-dimensional problem reduced to the two-dimensional one. To develop a numerical method we divided the particle into rectangular parallelepipeds with a square base of size δ in the plane x, y and of height h and obtained approximate expressions for different parts of the energy function using the grid values of magnetization $\vec{M} = \{M_x, M_y, M_z\}$. We chose the cell size by considering two factors. One, the size of the cell should be smaller than the characteristic exchange length $\sqrt{J/M_s^2}$ (J is constant of exchange interaction) in order to describe the inhomogeneous magnetization correctly. Two, we cannot make it very small because of the computation time limitations. So in calculations value of cell δ was less than 20 nm. All calculations were carried out for parameters of Co: $J = 10^{-6}\,\text{erg/cm}$, $M_s = 1400\,\text{G}$ and $V_{\text{eff}} = 1.25\times10^{-16}\,\text{cm}^3$. We omitted magnetocrystalline anisotropy term in Eq. (2), assuming polycrystalline structure of the particle.

4. Results and discussion

The MFM-induced magnetization reversal in elliptical Co nanoparticles was first observed by Kleiber et al. [21] The particles were placed in an external demagnetizing field

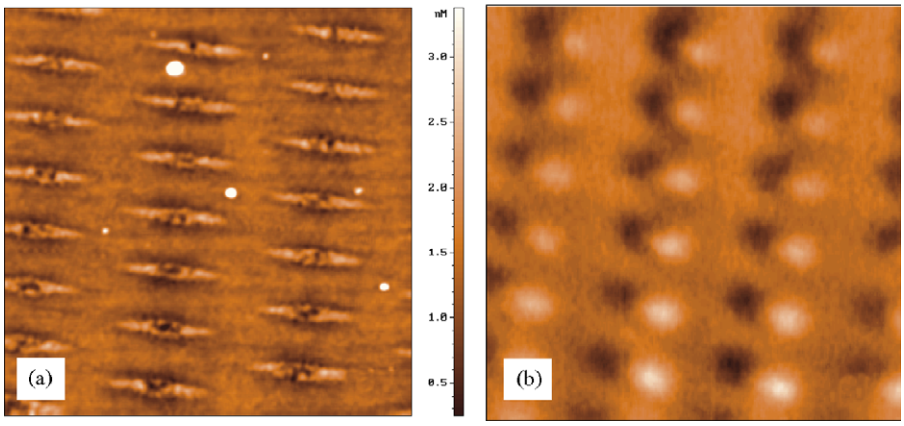

Fig. 1. AFM (a) and constant height MFM, (b) images of FeCr particles array. Scan area $4 \times 4\,\mu m$.

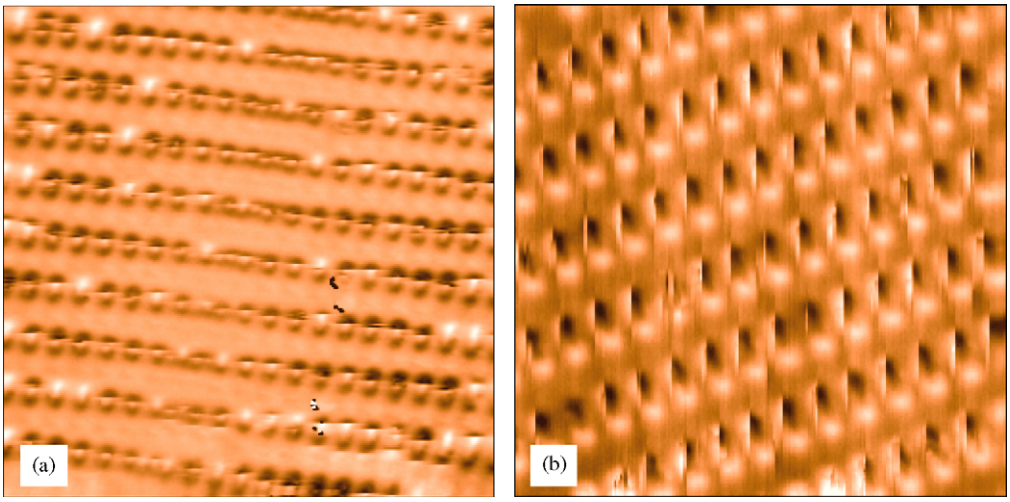

Fig. 2. FeCr particles array MFM images (tapping/lift mode) with different scan direction. Scan area $10 \times 10\,\mu m$ (a) and $8 \times 8\,\mu m$ (b).

less than the critical field and actually the MFM probe was used to initiate switching of magnetization between US with right (US_R) and left (US_L) orientation. Afterwards, authors [22,23] performed more detailed investigations showing that reorientation effects depend on the probe position relative to particle. They showed that the probe manipulation across the particle can lead to the magnetization reversal and, in particularly, possibility of one touch remagnetization by MFM probe with high magnetic moment was demonstrated. In the paper, we consider in detail magnetization reversal processes under an inhomogeneous magnetic field of MFM probe moving along the ferromagnetic particle.

We investigated MFM-induced magnetization reversal processes in the high aspect ratio $700\,nm \times 280\,nm$ FeCr particles. AFM and MFM (constant height mode) images of the sample are presented in Fig. 1. The particles have lentil-like shape clearly seen in Fig. 1(a). Separation between particles is about 500 nm. The sample was previously magnetized in the long-axis direction of the particle. The magnetic state of particles (Fig. 1(b)) shows the uniform distribution of magnetization. As was shown in the experiment, VS was not practically realized in these high aspect ratio particles. At the tapping/lift mode we observed practically 100% switching in magnetization direction of array elements (Fig. 2), which was characterized by sharp changing of MFM contrast during the tip scanning.

Micromagnetic simulations show that the reversal $US_R \Leftrightarrow US_L$ process is accompanied by a very complicated redistribution of particle magnetization. The step-by-step stages of remagnetization under MFM probe moving across the edge of a particle are presented in Fig. 3. The US_R was selected as the initial state (Fig. 3(a)). At the firs step, when the probe approaches the particle, part of magnetization vectors near the probe change their orientation under the influence of the probe magnetic field (Fig. 3(b)). In the next stage VS in the right part of the particle is formed (Fig. 3(c)). As the probe moves to the central part vortex-like state is formed (Fig. 3(d)), which breaks up the spin flip in the bottom part of particle (Fig. 3(e)). Finally, we have US_L with opposite direction of magnetization. This algorithm was used for manipulation of magnetic moment in separate selected particles. Tapping/lift mode or

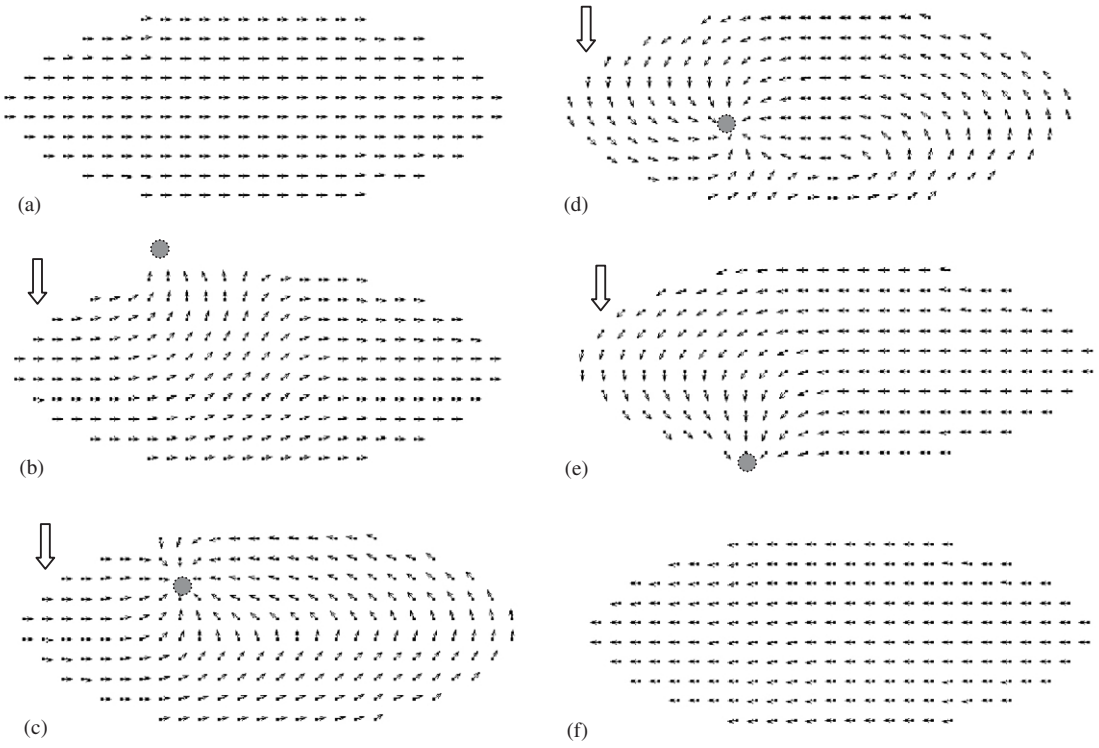

Fig. 3. Step-by-step stages of reversal $US_R \Leftrightarrow US_L$ process under MFM probe moving across the particle (the probe position indicated by a gray circle, scan direction indicated by an arrow).

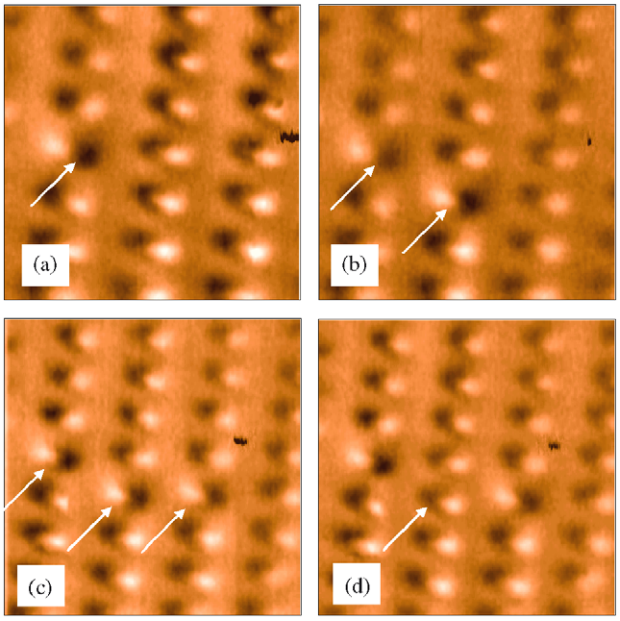

Fig. 4. Stages of tip-induced magnetization reversal process in Fe–Cr nanoparticles. Scan area $4.5 \times 4.5\,\mu m$.

constant height mode (with low scan height) scanning within one particle area was performed for switching of magnetization. The results of successive remagnetization of three particles are shown in Fig. 4. First, one particle was switched (shown by an arrow in Fig. 4(a)), then second (Fig. 4(b)) and third one subsequently (Fig. 4(c)). After that, the second particle was switched to the initial state (Fig. 4(d)).

So, the process can be used to control local magnetic field configuration in arrays of magnetic nanoparticles. For this purpose, one-dimensional arrays (chains) of elliptical Co particles with long axis perpendicular to the chain direction were fabricated near the Josephson junction [26]. The characteristic lateral sizes of particles were varied in the range 100–600 nm, separation between particles was 100–500 nm. As was observed, the distribution of magnetic moments of particles in the one-dimensional chain strongly depends on the interparticle distance. When the separation of chain is less than 100 nm, we observed antiferromagnetic ordering of moments of particles in the remanent state. It is a result of close magnetostatic interaction between particles. This interaction leads to unusual behavior of the system. We prepared another chain structure where individual ferromagnetic particle has lateral size of 300×150 nm with a height of 10 nm being separated by 150 nm. After magnetizing in the external field of 10 kOe in the direction parallel to the long axis, this chain has ferromagnetic ordering as shown in the MFM image (Fig. 5(a)). In this state, chain of particles have averaged magnetic field.

The probe-induced antiferromagnetic ordering of this chain was performed in constant height mode. The height of scanning was reduced over selected particles until magnetic moment changed to opposite direction. The distribution of local magnetic moments in particles after

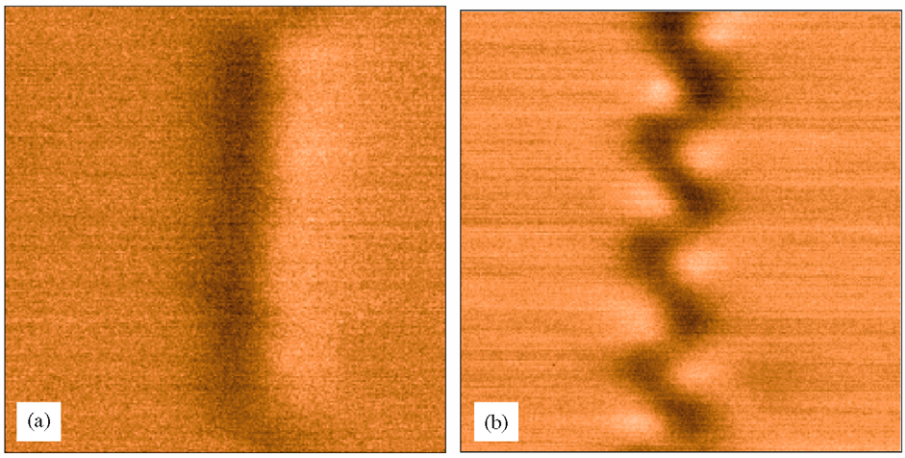

Fig. 5. MFM images of chain of particles after magnetizing in of 10 kG external field (a) and after probe-induced antiferromagnetic ordering (b). Scan area $3.5 \times 3.5\,\mu m$.

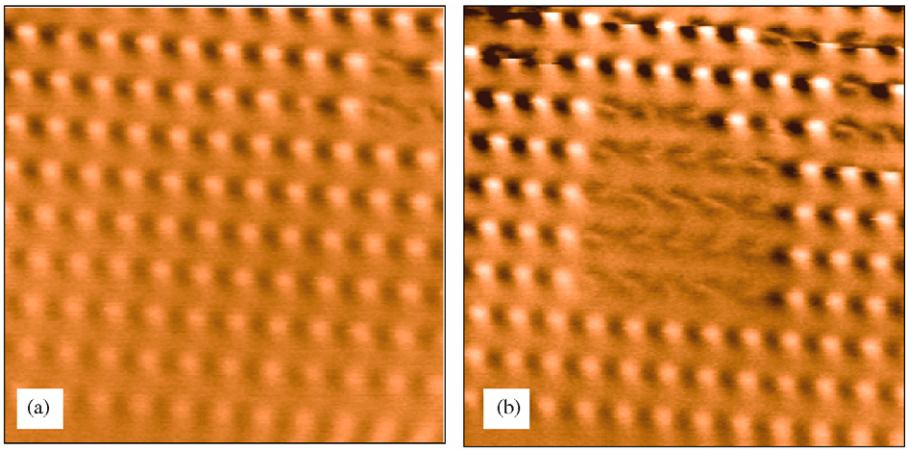

Fig. 6. Manipulation of local magnetization of individual magnetic nanodots using MFM tip-induced magnetization (a) most nanodot shows single-domain state except some dots at the upper right region (b) single-domain to single-vortex transition happens at the center by approaching a MFM tip.

probe-induced antiferromagnetic ordering can be clearly seen in Fig. 5(b). With the magnetic configuration, the normalized magnetic field of particles row is equal to zero.

The MFM probe-induced US $\Rightarrow$ VS transitions were used to control local magnetic field configuration in arrays of magnetic nanoparticles. For this purpose two-dimensional arrays of elliptical Co particles were formed. The characteristic lateral sizes of particles are 300×600 nm with a height of 25 nm. After magnetizing in 10 kOe external field in a direction to the long axis, all particles have uniform magnetization as is shown in the MFM image (Fig. 6(a)). In this state, array of particles induced sufficiently strong magnetic field. The probe-induced US $\Rightarrow$ VS demagnetization (transition to the VS with low magnetic field) in the selected area was performed in the tapping/lift mode. The distribution of local magnetic moments in particles after probe-induced US $\Rightarrow$ VS demagnetization is shown in the MFM image (Fig. 6(b)). In this state, magnetic field induced by the particles is very small.

In this way, we can control the magnetic state of individual ferromagnetic nanoparticles as well as create different distributions of local magnetic field. Tip-induced field switch on and switch off effects were already reported in the dependence of critical supercurrent of coplanar Josephson junction with ferromagnetic particles [11]. The same principle can be applied to control magnetic field in spintronic devices by means of switching of magnetic moment of particles grown over spin current channels.

5. Conclusion

In conclusion, we demonstrate the possibility to control the magnetic state of ferromagnetic nanoparticles by inhomogeneous magnetic field produced by a probe of MFM. The geometrical size and shape particle variations in combination with various methods of MFM probe manipulation allow to realize different $US_R \Leftrightarrow US_L$, US $\Leftrightarrow$ VS, transitions in magnetization distribution of the

particles. Computer calculations reveal that the process of magnetization reversal of ferromagnetic nanoparticles under the action of a magnetic probe has complicated character and scenario of the process, which is different in principle from the behavior of the system in homogeneous magnetic field. On the other hand, we formulated simple rules for manipulation of magnetic state of ferromagnetic nanoparticles using a probe of MFM and demonstrated possibilities for fabrication of different distributions of magnetic field induced by arrays of ferromagnetic nanoparticles. This is a very effective way to control switching properties of different objects. Therefore, we expected to apply this method to objects with strong magnetic susceptibility such as superconductors and semiconductors with giant Zeeman splitting.

Acknowledgments

This work was partly supported by Korea–Russia International Cooperation Program in KIST (2Z02660), RFBR, INTAS (03-51-6426, 03-51-4778), and ISTC (2976). The authors are very thankful to V.B. Shevtsov for help in MFM measurements, to N.I. Polushkin, YUKVerevkin for assistance in sample fabrication and to D.S. Nikitushkin, I.R. Karetnikova, I.M. Nefedov and I.A. Shereshevsky for assistance in computer simulations.

References

[1] J.I. Martin, J. Nogues, K. Liu, J.L. Vicent, I.K. Schuller, J. Magn. Magn. Mater. 256 (2003) 449.
[2] A.M. Kosevich, M.P. Voronov, I.V. Marjos, JETP Lett 84 (1) (1983) 148.
[3] R.P. Cowburn, D.K. Koltsov, A.O. Adeyeye, M.E. Welland, D.M. Tricker, Phys. Rev. Lett. 83 (1999) 1042.
[4] A. Fernandez, C.J. Cerjan, J. Appl. Phys. 87 (3) (2000) 1395.
[5] T. Okuno, K. Shigeto, T. Ono, K. Mibu, T. Shinjo, J. Magn. Magn. Mater. 240 (2002) 1.
[6] A.A. Fraerman, L. Belova, B.A. Gribkov, S.A. Gusev, A.Yu. Klimov, V.L. Mironov, D.S. Nikitushkin, G.L. Pakhomov, K.V. Rao, V.B. Shevtsov, M.A. Silaev, S.N. Vdovichev, Phys. Low — Dimens. Struct. 1/2 (2004) 35.
[7] Y. Otani, B. Pannetier, J.P. Nozieres, D. Givord, J. Magn. Magn. Mater. 126 (1993) 622.
[8] O. Geoffroy, D. Givord, Y. Otany, J. Magn. Magn. Mater. 121 (1993) 223.
[9] J.I. Martin, M. Velez, J. Nogues, I.K. Shuller, Phys. Rev. Lett. 79 (1997) 1929.
[10] A.V. Silhanek, L. Van Look, S. Raedts, R. Jonckheere, V.V. Moshchalkov, Phys. Rev. B. 68 (2003) 214504.
[11] A.Y. Aladyshkin, A.A. Fraerman, S.A. Gusev, A.Y. Klimov, Y.N. Nozdrin, G.L. Pakhomov, V.V. Rogov, S.N. Vdovichev, J. Magn. Magn. Mater. 258–259 (2003) 406.
[12] S.N. Vdovichev, B.A. Gribkov, S.A. Gusev, E. Il'ichev, Yu.N. Nozdrin, G.L. Pakhomov, A.V. Samokhvalov, R. Stolz, A.A. Fraerman, J. Magn. Magn. Mater. 300 (2006) 202.
[13] S.N. Vdovichev, B.A. Gribkov, S.A. Gusev, E. Il'ichev, A.Yu. Klimov, Yu.N. Nozdrin, G.L. Pakhomov, V.V. Rogov, R. Stolz, A.A. Fraerman, JETP Lett. 80 (2004) 651.
[14] M. Berciu, B. Janko, Phys. Rev. Lett. 90 (2003) 246804.
[15] T. Dietl, M. Sawicki, M. Dahl, D. Heiman, E.D. Isaacs, M.J. Graf, S.I. Gubarev, D.L. Alov, Phys. Rev. B 43 (1991) 3154.
[16] R. Merservey, D. Paraskevopoulos, P.M. Tedrow, Phys. Rev. B 22 (1980) 1331.
[17] V.A. Vas'ko, V.A. Larkin, P.A. Kraus, K.R. Nikolaev, D.E. Grupp, C.A. Nordman, A.M. Goldman, Phys. Rev. Lett. 78 (1997) 1134.
[18] F.J. Jedema, M.S. Nijboer, A.T. Filip, B.J. van Wees, Phys. Rev. B 67 (2003) 085319.
[19] V.V. Ryazanov, V.A. Oboznov, A.S. Prokofiev, S.V. Dubonos, JETP Lett. 77 (2003) 39.
[20] I. Zutic, J. Fabian, S. Das Sarma, Rev. Mod. Phys. 76 (2004) 323.
[21] M. Kleiber, F. Kümmerlen, M. Löhndorf, A. Wadas, D. Weiss, R. Wiesendanger, Phys. Rev. B 58 (2002) 5563.
[22] X. Zhu, P. Grütter, V. Metlushko, B. Ilic, Phys. Rev. B 66 (2002) 024423.
[23] X. Zhu, P. Grütter, V. Metlushko, B. Ilic, J. Appl. Phys. 91 (2002) 7340.
[24] M. Shneider, H. Hofman, J. Zweck, Appl. Phys. Lett. 79 (2001) 3113.
[25] A.A. Fraerman, S.A. Gusev, L.A. Mazo, I.M. Nefedov, Yu.N. Nozdrin, I.R. Karetnikova, M.V. Sapozhnikov, I.A. Shereshevsky, L.V. Sukchodoev, Phys. Rev. B 65 (2002) 064424.
[26] A.A. Fraerman, M.V. Sapozhnikov, Phys. Rev. B 65 (2002) 184433.